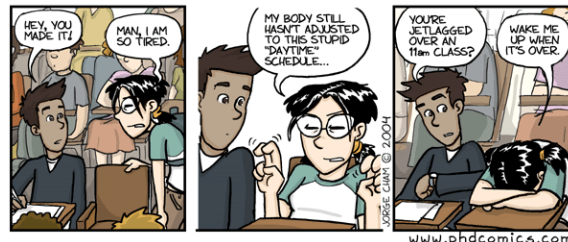
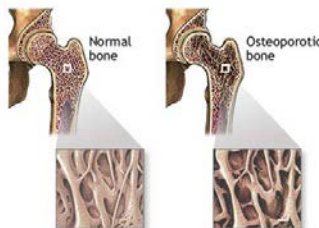


13 - basic constitutive equations - growing bones



13 - constitutive equations

1



osteoporosis

osteoporosis is a disease of bones that leads to an increased risk of fracture. osteoporosis literally means porous bones. in osteoporosis the bone mineral density is reduced, bone microarchitecture is disrupted, and the amount of variety of proteins in bone is altered. the diagnosis of osteoporosis can be made using conventional radiography. bone mineral density can be measured by dual energy x-ray absorptiometry, dxa or dexa. osteoporosis can be prevented with lifestyle changes and sometimes medication. lifestyle changes include exercise and preventing falls as well as reducing protein intake which may cause calcium to be taken from the bones.



motivation - growing bone

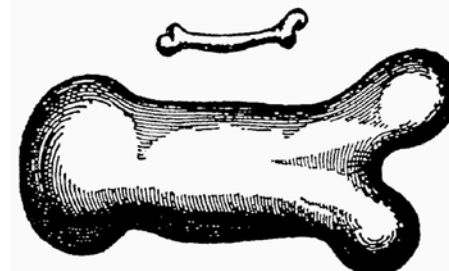
3

day	date	topic
tue	jan 08	motivation - everything grows!
thu	jan 10	basics maths - notation and tensors
tue	jan 15	basic kinematics - large deformation and growth
thu	jan 17	kinematics - growing hearts
tue	jan 22	guest lecture - growing surfaces
thu	jan 24	kinematics - growing leaflets
tue	jan 29	basic balance equations - closed and open systems
thu	jan 31	basic constitutive equations - growing muscle
tue	feb 05	basic constitutive equations - growing tumors
thu	feb 07	volume growth - finite elements for growth - theory
tue	feb 12	volume growth - finite elements for growth - matlab
thu	feb 14	volume growth - growing skin
tue	feb 19	basic constitutive equations - growing bones
thu	feb 21	density growth - finite elements for growth
tue	feb 26	density growth - growing bones
thu	feb 28	everything grows! - midterm summary
tue	mar 05	midterm
thu	mar 07	remodeling - remodeling arteries and tendons
tue	mar 12	class project - discussion, presentation, evaluation
thu	mar 14	class project - discussion, presentation, evaluation
thu	mar 14	written part of final projects due

where are we???

2

history - 17th century



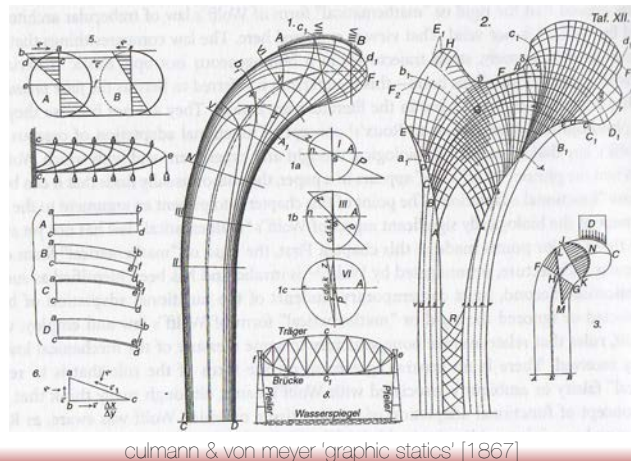
...dal che e manifesto, che chi volesse mantener in un vastissimo gigante le proporzioni, che hanno le membra in un huomo ordinario, bisognerebbe o trouar materia molto piu dura, e resistente per formarne l'ossa o vero ammettere, che la robustezza sua fusse a proporzioni assai piu fiaca, che negli huomini de statura mediocre; altrimenti crescendogli a smisurata altezza si vedrebbono dal proprio peso opprimere, e cadere...'

galileo, 'discorsi e dimostrazioni matematiche', [1638]

introduction

4

history - 19th century

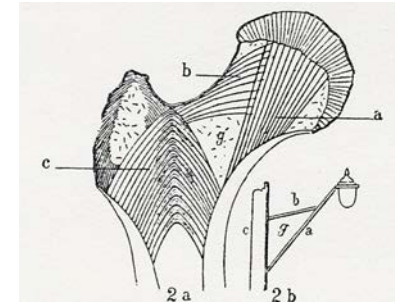


culmann & von meyer 'graphic statics' [1867]

motivation - growing bone

5

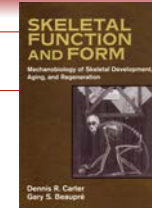
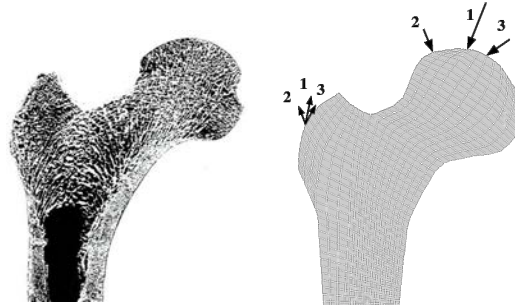
history - 19th century



„...es ist demnach unter dem gesetze der transformation der knochen dasjenige gesetz zu verstehen, nach welchem im gefolge primärer abänderungen der form und inanspruchnahme bestimmte umwandlungen der inneren architectur und umwandlungen der äusseren form sich vollziehen...“

wolff 'gesetz der transformation der knochen' [1892]

different load cases



- [1] midstance phase of gait 2317 N 24° 703 N 28°
- [2] extreme range of abduction 1158 N -15° 351 N -8°
- [3] extreme range of adduction 1548 N 56° 468 N 35°

carter & beaupré [2001]

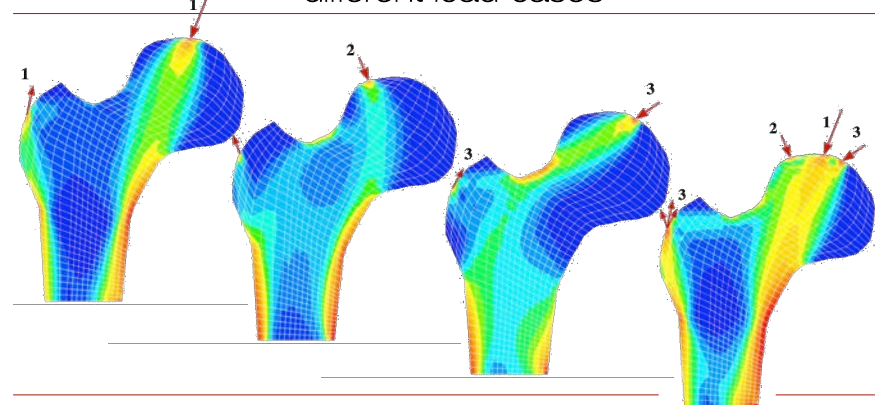
motivation - growing bone

7

motivation - growing bone

6

different load cases



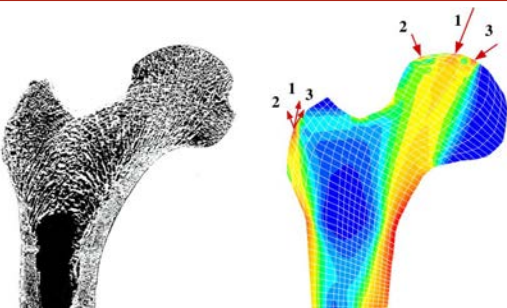
only combination of all load cases predicts profile

carter & beaupré [2001]

motivation - growing bone

8

experiment vs simulation



- dense system of compressive trabaculae carrying stress into calcar region
- secondary arcuate system, medial joint surface to lateral metaphyseal region
- ward's triangle, low density region contrasting dense cortical shaft

carter & beaupré [2001]

motivation - growing bone

9

 Modeling Bone Growth in High-Performance Tennis Players

Rebecca Taylor^a, Chunhua Zheng^b, Ryan Jackson^{a*}, Joey Doll^b, Amir Shamloo^b, Ellen Kuhl^a
Stanford University^a, Stanford School of Medicine^b

Purpose
It is well known that exercise-induced loads cause bone hypertrophy in the dominant arm of tennis players; this phenomenon has been documented by numerous studies of players who began play at pre-pubescent ages¹. However, the details about the processes of growth and remodeling that accompany this observation are unknown.^{2,3}

In addition, it is unclear as to which are the dominant variables that shape bone growth, muscular loading, impact forces during play or biological factors. We hypothesize that we can model this bone hypertrophy using a finite element growth model and that simulation gives further insight into the interplay between load and biological response.

Methods
The humerus was chosen for our study because it is the least complex of the arm bones. We investigated various loading scenarios and found tennis players to be excellent subjects because they show asymmetrical bone growth, and bone size in the non-dominant arm can be used as a control. We hypothesize that peak loading conditions occur during the high-speed serve. Based on video observation of tennis serves, we determined a posture for peak humerus stress. From this, approximate muscle forces were calculated with OpenSim. These forces were applied as external loads in a finite element growth model developed in class.

Results
A three dimensional finite element model of the human humerus has been generated. Three dimensional muscle force vectors, muscle attachment points and boundary conditions for the finite element simulation have been determined based on video analysis with the help of OpenSim. The results of the simulation of the serve on shear energy driven bone growth reveals pronounced twisted increase in bone mass density in the dominant right arm. The results of the simulation of Figure 6 are in qualitatively good agreement with the bone mass density scans displayed in Figure 1.

Figure 2: Observation of serve posture suggests that humerus remains aligned with shoulders throughout serve. Humerus rotation is identified as most critical motion influencing bone growth in tennis players.

Figure 3: Critical serve posture at moment of racket-ball contact.

Figure 4: Meshed humerus in OpenSim (left) and finite element mesh (right) with 1182 nodes and 4362 linear tetrahedral elements, muscle forces approximated with OpenSim.

Figure 5: Density changes with increasing number of load cycles.

Figure 6: Variation in humerus density in left and right arm of professional tennis player: Finite element simulation.

Conclusions
The encouraging results of our study could be of equal benefit to high performance athletes and patients with degenerative bone diseases. Based on patient-specific studies, optimized training strategies can be developed to promote bone growth.

Acknowledgments
We would like to thank Thor Besier for sharing his images, video, and density study data with us. Many thanks to Scott Delp for granting us access to OpenSim and Kate Holzbaur for sharing her upper limb model with us and for graciously assisting us throughout our study.

References

- Jones HH, Priest JO, Hayes WC, Tichner CA, Nagel DA. Humeral hypertrophy in response to weight-bearing exercise. *Am J Phys Med* 1971;50:171-175.
- Pearson OM, Lusk J, Lusk C. The aging of Wolff's Law?: Ontogeny and responses to mechanical loading in cortical bone. *Yearbook Phys Anthro* 2004;47:63-96.
- Shamloo A, Gholipour M, Jackson R, Kuhl E, Amiz C, Carter DR. Numerical instabilities in bone remodelling simulations. *J Biomech* 1995;28:445-450.

http://biomechanics.stanford.edu/mechanics_of_growth <https://simtk.org/home/simgrowth>

class project - me337 - mechanics of growth

rebecca e. taylor

neuromuscular
biomechanics lab

joseph c. doll

scott delp

amir shamloo

kate holzbaur

ryan p. jackson

human
performance lab

chun hua zheng

thor bezier



inter-arm asymmetry in high performance tennis players

example - twisted tennis arm density

10

The phenomenon of twisted growth: humeral torsion in dominant arms of high performance tennis players

R.E. Taylor^a, C. Zheng^a, R.P. Jackson^b, J.C. Doll^b, J.C. Chen^b, K.R.S. Holzbaur^c, T. Besier^d and E. Kuhl^{ab*}

^aDepartment of Mechanical Engineering, Stanford University, Stanford, CA, USA; ^bDepartment of Bioengineering, Stanford University, Stanford, CA, USA; ^cDepartment of Biomedical Engineering, Wake Forest University School of Medicine, Winston-Salem, NC, USA;

^dDepartment of Orthopaedic Surgery, Stanford University, Stanford, CA, USA

(Received 27 November 2007; final version received 2 May 2008)

This manuscript is driven by the need to understand the fundamental mechanisms that cause twisted bone growth and shoulder pain in high performance tennis players. Our ultimate goal is to predict bone mass density in the humerus through computational analysis. The underlying study spans a unique four level complete analysis consisting of a high-speed video analysis, a musculoskeletal analysis, a finite element based density growth analysis and an X-ray based bone mass density analysis. For high performance tennis players, critical loads are postulated to occur during the serve. From high-speed video analyses, the serve phases of maximum external shoulder rotation and ball impact are identified as most critical loading situations for the humerus. The corresponding posts from the video analysis are reproduced with a musculoskeletal analysis tool to determine muscle attachment points, muscle force vectors and overall forces of relevant muscle groups. Collective representative muscle forces of the deltoid, latissimus dorsi, pectoralis major and triceps are then applied as external loads in a fully 3D finite element analysis. A problem specific nonlinear finite element based density analysis tool is developed to predict functional adaptation over time. The density profiles in response to the identified critical muscle forces during serve are qualitatively compared to X-ray based bone mass density analyses.

Keywords: bone mass density changes; functional adaptation; musculoskeletal analysis; finite element analysis; sports medicine

example - twisted tennis arm density

12

The Stanford Daily

An Independent Publication

If there's one thing that's guaranteed, it's that Jeff Zeller strives to apply what he knows in various contexts. Whether it be while injured, in doubles or in singles matches, the sophomore will take his wisdom and work to develop his game.

Although the Zeller redshirted in 2006 because of injury, he was still able to observe his teammates in action and apply this knowledge to his own game when he returned to the court.

This year, Zeller has used this experience, and along with senior Eric McKean, has formed a successful doubles pair that draws inspiration from the Bryan brothers (Bob and Mike Bryan — both former Stanford players).

Throughout this season, Zeller has learned to apply doubles tactics in order to improve his singles game, too. These circumstances demonstrate why head coach John Whittington will attest to the fact that the Centennial, Colo. native is such a "good student of the game."

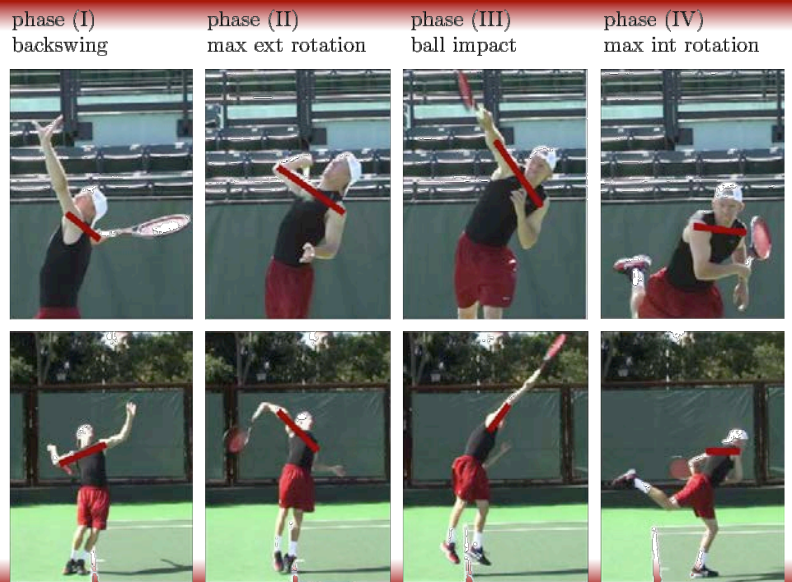
Zeller injured his hand in January of 2006 and took three months off from tennis. Even when Zeller started hitting again in the spring, he was not at 100 percent and, therefore, could not practice with the team. In his first year on The Farm, Zeller was forced into the role of an onlooker and was not able to contribute to the team on the court.

"When I got injured, I took on more of the observer role, but I got to watch my teammates succeed," Zeller said. "I got to watch [sophomore] Matt [Bruch] get ranked top 5 in the country; I got to watch KC [Corke] get to the semifinals of NCAAs; I got to watch KC and [then-senior] James Fadé play some amazing doubles. I think I really learned a lot from just sitting back and seeing what my teammates did well that allowed them to be successful."



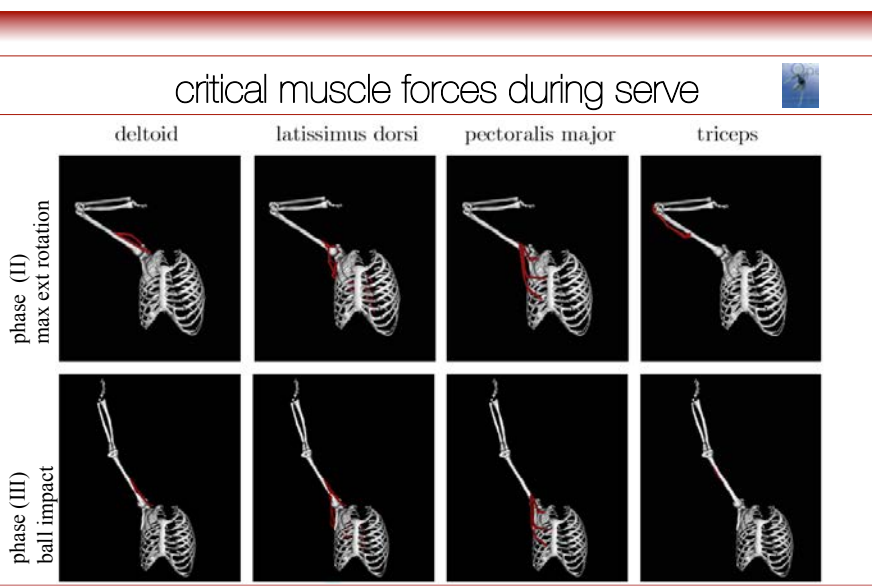
example - twisted tennis arm density

13



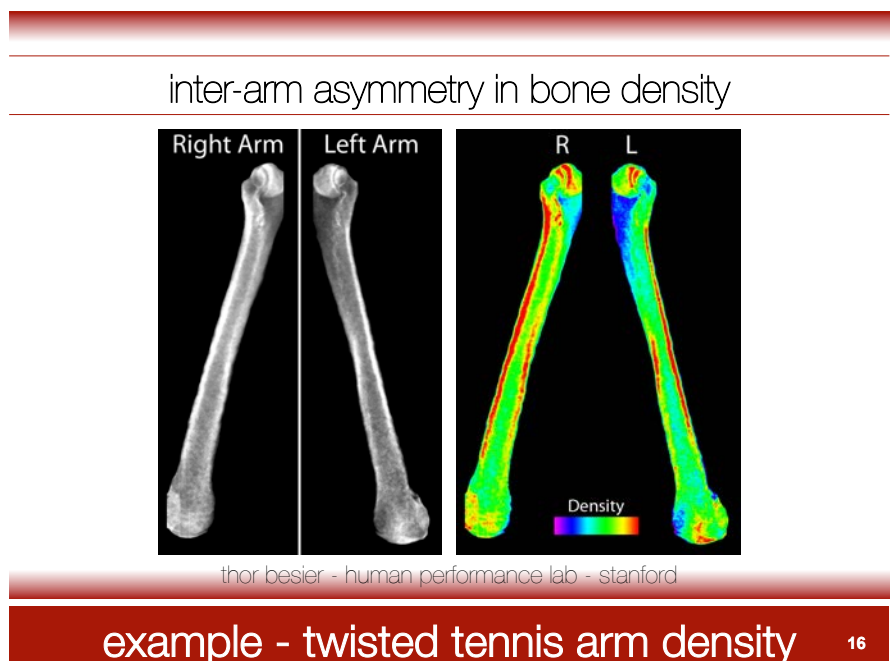
example - twisted tennis arm density

14



example - twisted tennis arm density

15

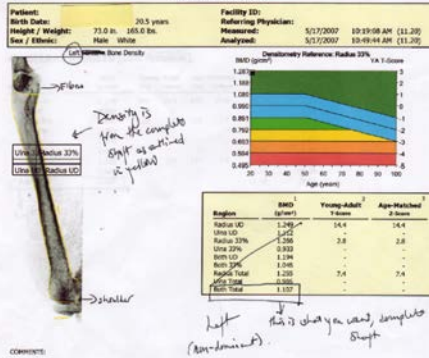


example - twisted tennis arm density

16

inter-arm asymmetry in bone density

Stanford University Sports Medicine Clinic
341 Galvez Street
Stanford, CA 94305



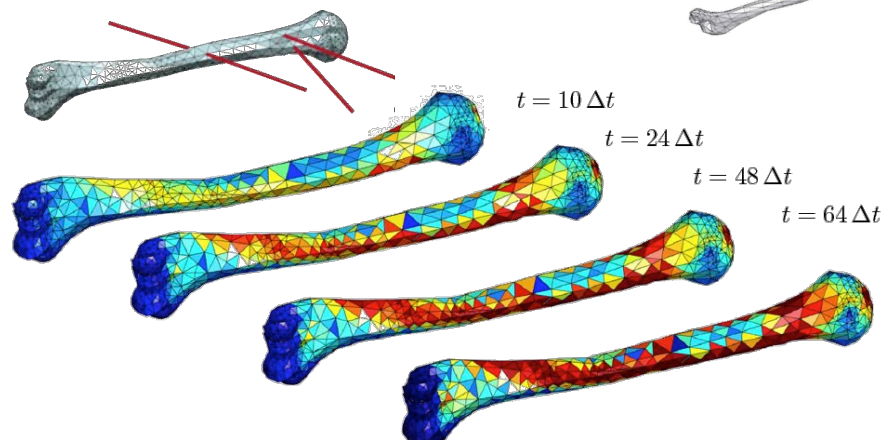
bmd left 1.107 g/mm^2

bmd right 1.369 g/mm^2

example - twisted tennis arm density

17

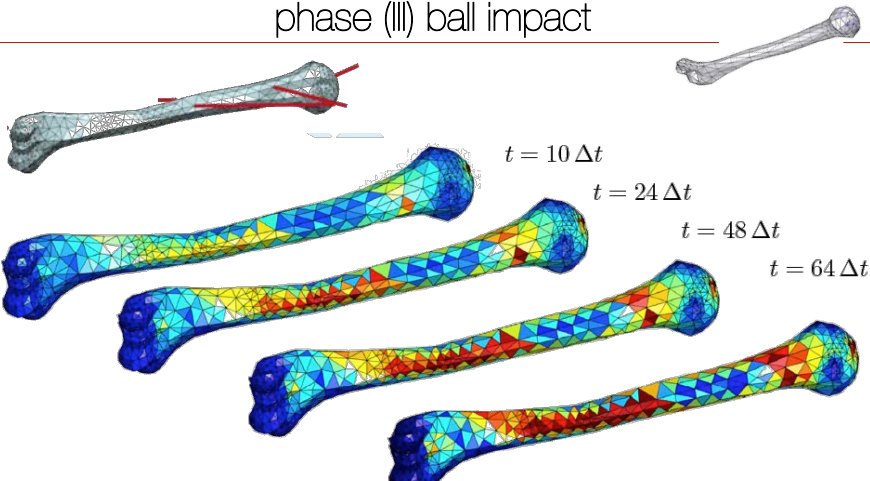
phase (II) maximum external shoulder rotation



example - twisted tennis arm density

18

phase (III) ball impact



example - twisted tennis arm density

19

pitcher's arm



a physical-conditioning program for pitchers is geared to striking a balance between muscle strength and endurance, tendon/ligament strength and flexibility, and optimal cartilage and **bone density**. bone hypertrophy occurs in response to physical activity. the bones in the throwing arm of a baseball pitcher are **denser and thicker** than those of the other arm. bone hypertrophy is **stimulated by the magnitude of loading** rather than by the frequency.

example – pitcher's arm

20

pitcher's arm

the real secret to tim lincecum's overpowering velocity is all **stored within his pitching mechanics**. it has little to do with his size and strength. six things in tim lincecum's pitching delivery create his amazing arm speed:

- move fast from back leg to front leg
- use back leg to move out very low to ground
- get throwing arm up very late in delivery
- stride length of over 100% of pitcher's height
- brace front leg to increase upper body speed
- land in a straight line toward plate

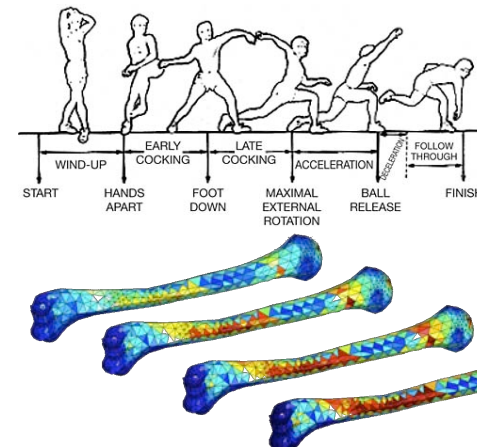


tim lincecum's pitching mechanics, because he moves fast into a long stride and stays low, forces his body to **put as many muscles on stretch as quickly as possible** which helps develop **maximum elastic energy** so that **his body acts like a huge rubber band** stretching to its maximum length ready to be let go and whip the arm through.

example – pitcher's arm

21

pitcher's arm

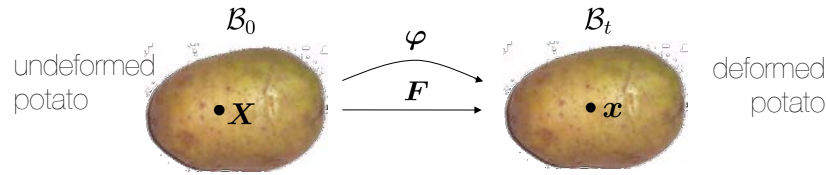


maximal external shoulder rotation stimulates twisted density growth

example – pitcher's arm

22

neo hooke'ian elasticity of solid materials



- free energy $\psi_0^{\text{neo}} = \frac{1}{2} \lambda_0 \ln^2(\det(\mathbf{F})) + \frac{1}{2} \mu_0 [\mathbf{F}^t \cdot \mathbf{F} : \mathbf{I} - n^{\text{dim}} - 2 \ln(\det(\mathbf{F}))]$

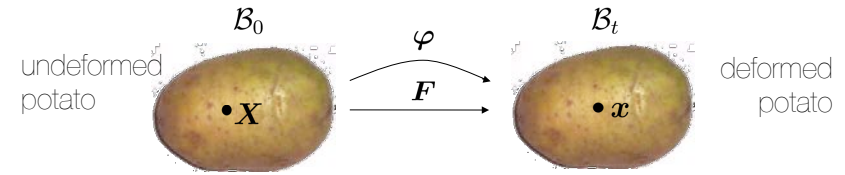
- definition of stress

$$\mathbf{P}^{\text{neo}} = D_F \psi_0^{\text{neo}} = \mu_0 \mathbf{F} + [\lambda_0 \ln(\det(\mathbf{F})) - \mu_0] \mathbf{F}^{-t}$$

constitutive equations

23

neo hooke'ian elasticity of solid materials



- free energy $\psi_0^{\text{neo}} = \frac{1}{2} \lambda_0 \ln^2(\det(\mathbf{F})) + \frac{1}{2} \mu_0 [\mathbf{F}^t \cdot \mathbf{F} : \mathbf{I} - n^{\text{dim}} - 2 \ln(\det(\mathbf{F}))]$

- large strain - lamé parameters and bulk modulus

$$\lambda = \frac{E\nu}{[1+\nu][1-2\nu]} \quad \mu = \frac{E}{2[1+\nu]} \quad \kappa = \frac{E}{3[1-2\nu]}$$

- small strain – young's modulus and poisson's ratio

$$E = 3\kappa [1 - 2\nu] \quad \nu = \frac{3\kappa - 2\mu}{2[3\kappa + \mu]}$$

constitutive equations

24

neo hooke'ian elasticity of solid materials

- free energy $\psi_0^{\text{neo}} = \frac{1}{2} \lambda_0 \ln^2(\det(\mathbf{F})) + \frac{1}{2} \mu_0 [\mathbf{F}^t \cdot \mathbf{F} : \mathbf{I} - n^{\text{dim}} - 2 \ln(\det(\mathbf{F}))]$

- definition of stress

$$\begin{aligned}\mathbf{P}^{\text{neo}} &= \mathbf{D}_F \psi_0^{\text{neo}} \\ &= \frac{1}{2} \lambda_0 2 \ln(\det \mathbf{F}) \mathbf{F}^{-t} + \frac{1}{2} \mu_0 2 \mathbf{F} - \mu_0 \mathbf{F}^{-t} \\ &= \mu_0 \mathbf{F} + [\lambda_0 \ln(\det(\mathbf{F})) - \mu_0] \mathbf{F}^{-t}\end{aligned}$$

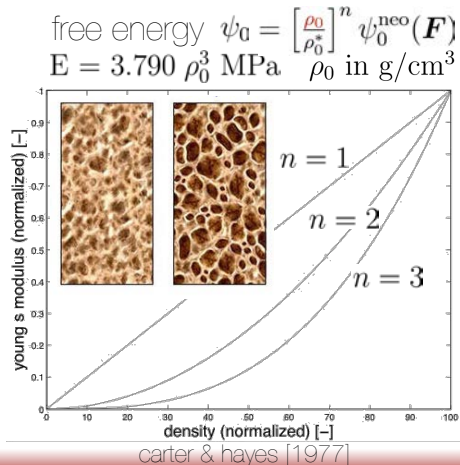
- definition of tangent operator

$$\begin{aligned}\mathbf{A}^{\text{neo}} &= \mathbf{D}_{FF} \psi_0^{\text{neo}} = \mathbf{D}_F \mathbf{P}^{\text{neo}} \\ &= \lambda_0 \mathbf{F}^{-t} \otimes \mathbf{F}^{-t} + \mu_0 \mathbf{I} \otimes \mathbf{I} \\ &\quad + [\mu_0 - \lambda_0 \ln(\det(\mathbf{F}))] \mathbf{F}^{-t} \otimes \mathbf{F}^{-1}\end{aligned}$$

constitutive equations

25

neo hooke'ian elasticity of cellular materials



constitutive equations

27

neo hooke'ian elasticity of solid materials

- free energy $\psi_0^{\text{neo}} = \frac{1}{2} \lambda_0 \ln^2(F_{ij}) + \frac{1}{2} \mu_0 [F_{ij} F_{ji} - n^{\text{dim}} - 2 \ln(F_{ij})]$

- definition of stress

$$\begin{aligned}P_{ij}^{\text{neo}} &= \mathbf{D}_{F_{ij}} \psi_0^{\text{neo}} \\ &= \frac{1}{2} \lambda_0 2 \ln(\det F_{ij}) F_{ji}^{-1} + \frac{1}{2} \mu_0 2 F_{ij} - \mu_0 F_{ji}^{-1} \\ &= \mu_0 F_{ij} + [\lambda_0 \ln(\det(F_{ij})) - \mu_0] F_{ji}^{-1}\end{aligned}$$

- definition of tangent operator

$$\begin{aligned}\mathbf{A}_{ijkl}^{\text{neo}} &= \mathbf{D}_{F_{ij} F_{kl}} \psi_0^{\text{neo}} = \mathbf{D}_{F_{kl}} P_{ij}^{\text{neo}} \\ &= \lambda_0 F_{ji}^{-1} F_{lk}^{-1} + \mu_0 I_{ik} I_{jl} \\ &\quad + [\mu_0 - \lambda_0 \ln(\det(F_{ij}))] F_{li}^{-1} F_{jk}^{-1}\end{aligned}$$

constitutive equations

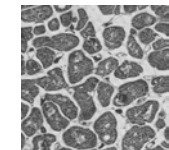
26

open systems - balance of mass

$$D_t \rho_0 = \text{Div}(\mathbf{R}) + \mathcal{R}_0$$

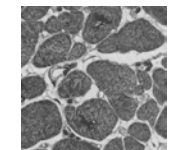
mass flux \mathbf{R}

- cell movement (migration)



mass source \mathcal{R}_0

- cell growth (proliferation)
- cell division (hyperplasia)
- cell enlargement (hypertrophy)



biological equilibrium

cowin & hegedus [1976], beaupré, orr & carter [1990], harrigan & hamilton [1992], jacobs, levenson, beaupré, simo & carter [1995], huiskes [2000], carter & beaupré [2001]

balance equations

28

open systems - balance of momentum

- volume specific version

$$D_t(\rho_0 \mathbf{v}) = \text{Div}(\mathbf{P} + \mathbf{v} \otimes \mathbf{R}) + [\mathbf{b}_0 + \mathbf{v}\mathcal{R}_0 - \nabla_X \mathbf{v} \cdot \mathbf{R}]$$

- subtraction of weighted balance of mass

$$\mathbf{v} D_t \rho_0 = \text{Div}(\mathbf{v} \otimes \mathbf{R}) + \mathbf{v}\mathcal{R}_0 - \nabla_X \mathbf{v} \cdot \mathbf{R}$$

- mass specific version

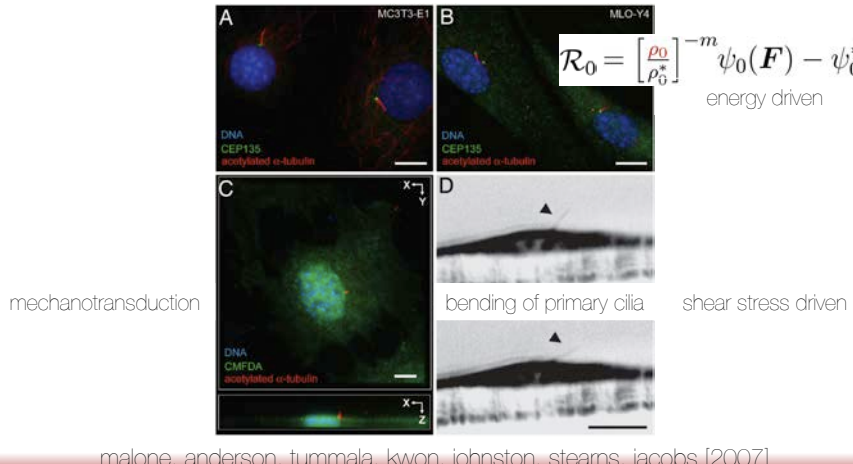
$$\rho_0 D_t \mathbf{v} = \text{Div}(\mathbf{P}) + \mathbf{b}_0$$

mechanical equilibrium

balance equations

29

driving force for density growth - why does bone grow?

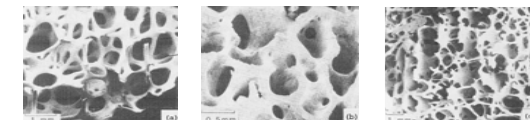


constitutive equations

31

density growth at constant volume

- free energy $\psi_0 = \left[\frac{\rho_0}{\rho_0^*} \right]^n \psi_0^{\text{neo}}(\mathbf{F})$
- stress $\mathbf{P} = \left[\frac{\rho_0}{\rho_0^*} \right]^n \mathbf{P}^{\text{neo}}(\mathbf{F})$
- mass flux $\mathbf{R} = R_0 \nabla_X \rho_0$
- mass source $\mathcal{R}_0 = \left[\frac{\rho_0}{\rho_0^*} \right]^{-m} \psi_0(\mathbf{F}) - \psi_0^*$



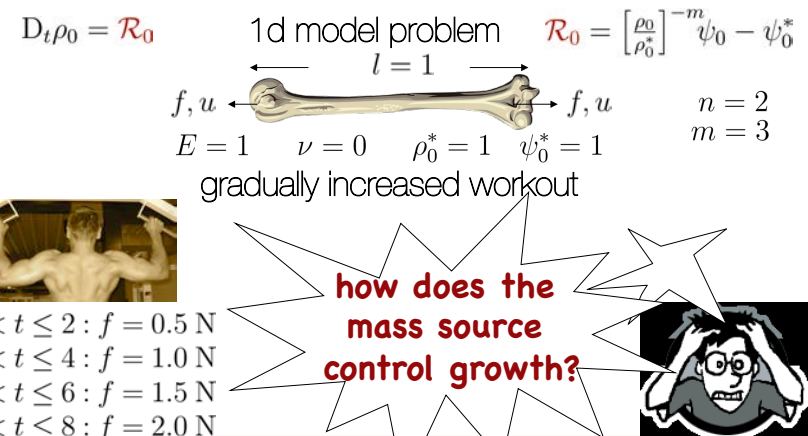
constitutive coupling of growth and deformation

gibson & ashby [1999]

constitutive equations

30

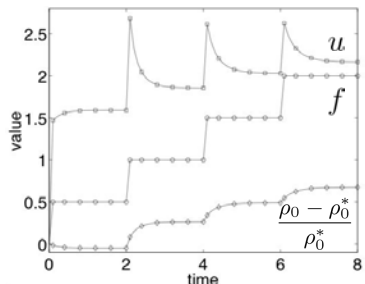
density growth - mass source



32

density growth - mass source

$$D_t \rho_0 = \mathcal{R}_0 \quad f \leftarrow \text{bone} \quad \mathcal{R}_0 = \left[\frac{\rho_0}{\rho_0^*} \right]^{-m} \psi_0 - \psi_0^*$$



$$\begin{array}{ll} f = 0.5 \text{ N} & u = 1.5910 l \\ f = 1.0 \text{ N} & u = 1.8559 l \\ f = 1.5 \text{ N} & u = 2.0310 l \\ f = 2.0 \text{ N} & u = 2.1652 l \\ \text{resorption} & -1 < \frac{\rho_0 - \rho_0^*}{\rho_0^*} < 0 \\ \text{growth} & 0 < \frac{\rho_0 - \rho_0^*}{\rho_0^*} < \infty \end{array}$$

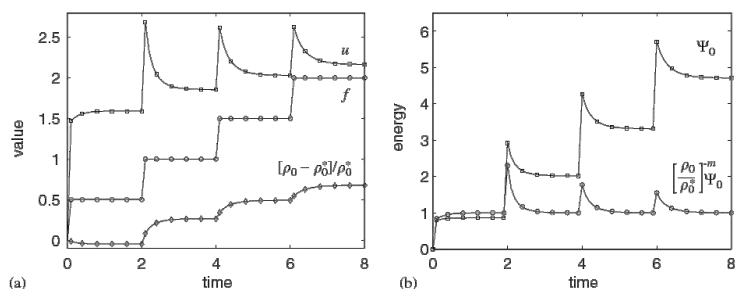
increasing force causes bone density increase

constitutive equations

33

density growth - mass source

$$D_t \rho_0 = \mathcal{R}_0 \quad f \leftarrow \text{bone} \quad \mathcal{R}_0 = \left[\frac{\rho_0}{\rho_0^*} \right]^{-m} \psi_0 - \psi_0^*$$



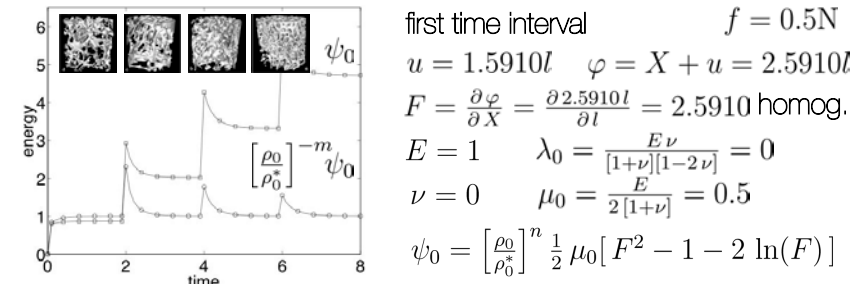
convergence towards biological equilibrium $D_t \rho_0 = 0$

constitutive equations

35

density growth - mass source

$$D_t \rho_0 = \mathcal{R}_0 \quad f \leftarrow \text{bone} \quad \mathcal{R}_0 = \left[\frac{\rho_0}{\rho_0^*} \right]^{-m} \psi_0 - \psi_0^*$$



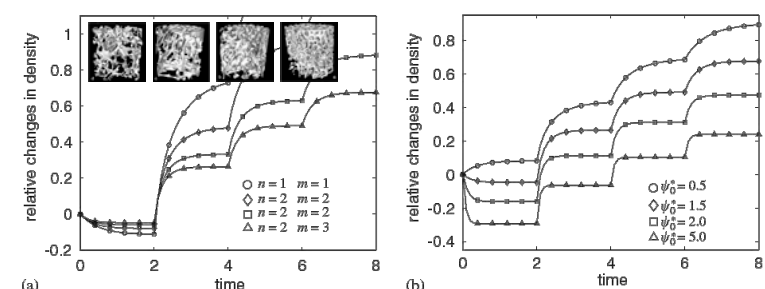
increasing force causes energy increase

constitutive equations

34

density growth - mass source

$$D_t \rho_0 = \mathcal{R}_0 \quad f \leftarrow \text{bone} \quad \mathcal{R}_0 = \left[\frac{\rho_0}{\rho_0^*} \right]^{-m} \psi_0 - \psi_0^*$$

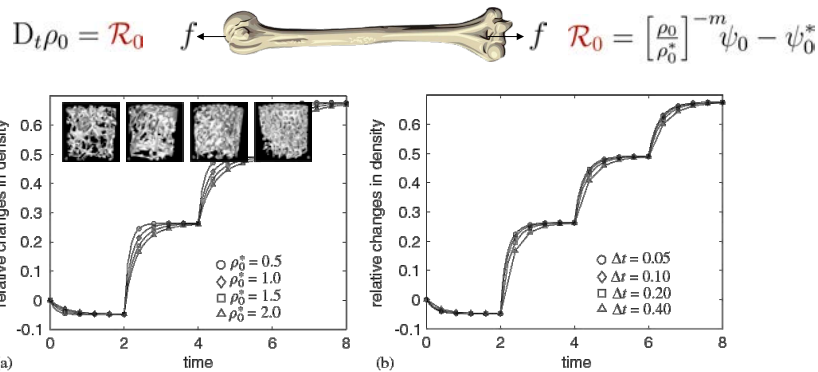


parameter sensitivity with respect to n, m, ψ_0^*

constitutive equations

36

density growth - mass source

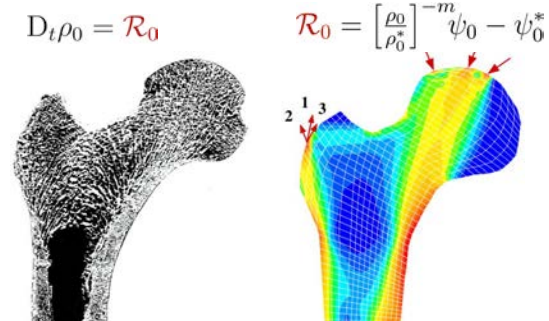


parameter insensitivity with respect to $\rho_0^*, \Delta t$

constitutive equations

37

density growth - mass source



the density evolves such that the tissue can just support the given mechanical load

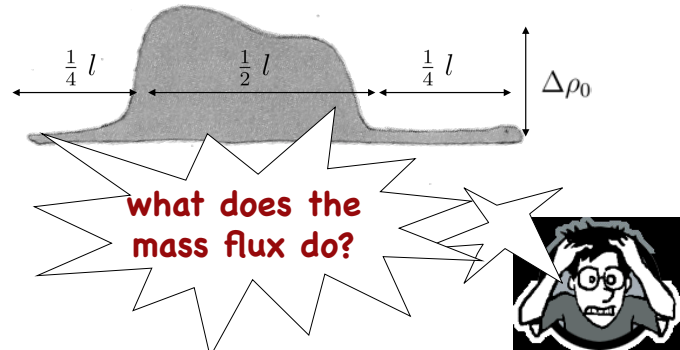
constitutive equations

38

density growth - mass flux

$$D_t \rho_0 = \text{Div}(\mathbf{R}) \quad \mathbf{R} = R_0 \nabla_X \rho_0$$

initial hat type density distribution



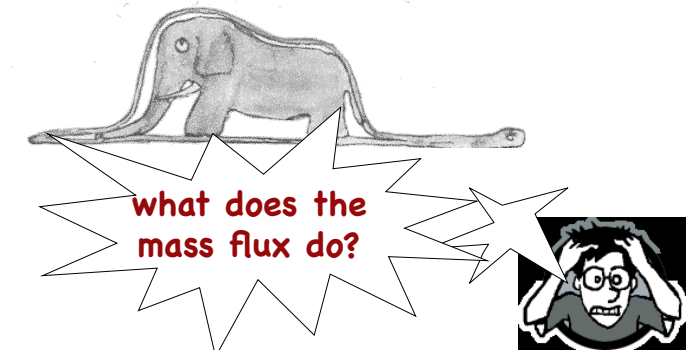
constitutive equations

39

density growth - mass flux

$$D_t \rho_0 = \text{Div}(\mathbf{R}) \quad \mathbf{R} = R_0 \nabla_X \rho_0$$

initial hat type density distribution

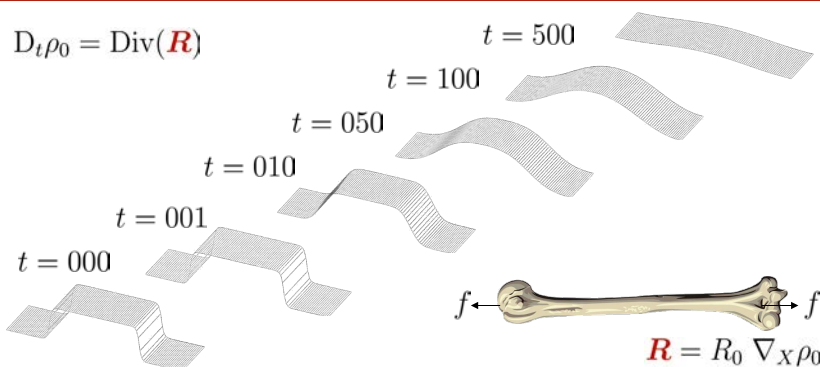


constitutive equations

40

density growth - mass flux

$$D_t \rho_0 = \text{Div}(\mathbf{R})$$



mass flux equilibrates concentrations

constitutive equations

41



density growth - bone loss in space



human space flight to mars could become a reality within the next 25 years, but not until some physiological problems are resolved, including an **alarming loss of bone mass, fitness and muscle strength**. gravity at mars' surface is about **38 percent** of that on earth. with lower gravitational forces, **bones decrease in mass and density**. the rate at which we lose bone in space is 10-15 times greater than that of a post-menopausal woman and there is no evidence that bone loss ever slows in space. further, it is not clear that space travelers will regain that bone on returning to gravity. during a trip to mars, lasting 13 and 30 months, unchecked bone loss could make an astronaut's skeleton the equivalent of a 100-year-old person.



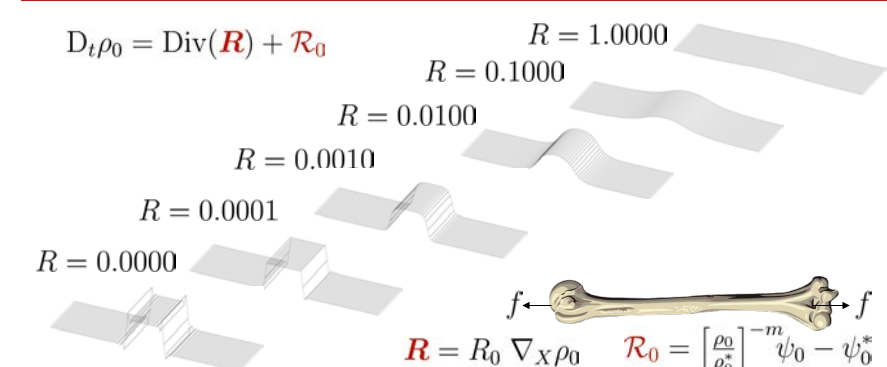
<http://www.acsm.org>

example - bone loss in space

43

density growth - mass flux & source

$$D_t \rho_0 = \text{Div}(\mathbf{R}) + \mathcal{R}_0$$



mass flux smoothes concentration profiles

constitutive equations

42



density growth - bone loss in space



$$D_t \rho_0 = \mathcal{R}_0 \quad \mathcal{R}_0 = c \frac{\rho_0}{\psi_0^*} [\psi_0 - \psi_0^*]$$

nasa has collected data that humans in space lose bone mass at a rate of $c = 1.5\%/\text{month}$. so far, **no astronauts have been in space for more than 14 months** but the predicted rate of bone loss seems constant in time. this could be a severe problem if we want to send astronauts on a **3 year trip to mars and back**. how long could an astronaut survive in a zero-g environment if we assume the critical bone density to be $\rho_0^{\text{crit}} = 1.00 \frac{\text{g}}{\text{cm}^3}$? you can assume an initial density of $\rho_0^* = 1.79 \frac{\text{g}}{\text{cm}^3}$!



example - bone loss in space

44

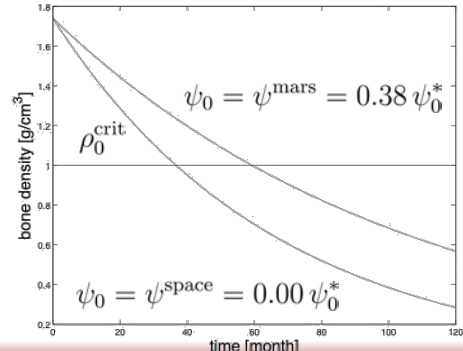


density growth - bone loss in space



$$D_t \rho_0 = c \rho_0 \left[\frac{\psi_0}{\psi_0^*} - 1 \right] \quad D_t \rho_0 = \frac{1}{\Delta t} [\rho_0^{n+1} - \rho_0^n]$$

$$\rho_0^{n+1} = \rho_0^n + c \rho_0^n \left[\frac{\psi_0}{\psi_0^*} - 1 \right] \Delta t \quad \rho_0(t_0) = 1.79 \frac{\text{g}}{\text{cm}^3}$$



$$\rho_0(36) = 1.0098$$

$$\rho_0(37) = 0.9947$$



example - bone loss in space

45

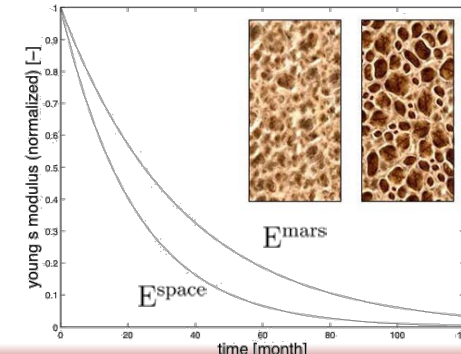


density growth - bone loss in space



$$E = 3.790 \rho_0^3 \text{ MPa} \quad \text{with } \rho_0 \text{ in g/cm}^3$$

carter & hayes [1977]



example - bone loss in space

46